# $Co_{core}Au_{shell}$ nanoparticles: evolution of magnetic properties in the displacement reaction

**Saikat Mandal and Kannan M. Krishnan***

***Received 14th September 2006, Accepted 26th October 2006***
***First published as an Advance Article on the web 14th November 2006***
**DOI: 10.1039/b613371c**

Development of simple and reliable protocols for the synthesis of phase-pure core–shell metal nanoparticles is an important problem in nanomaterials synthesis; the synthesis of Co-core Au-shell nanoparticles is described in this paper. The formation of these core–shell nanoparticles is driven by a displacement reaction on the surface of cobalt nanoparticles, where the surface of the cobalt nanoparticle is sacrificed sequentially as the reducing agent for the gold metal deposition on its surface. Hysteretic magnetic properties of nanoparticles depend critically on their size and since, in this displacement reaction, the size of the magnetic core decreases as a function of the displacement reaction time, we utilize it in a unique and systematic way to monitor the formation of the Co@Au core–shell morphology. In addition to magnetic measurements, synthesis of Co@Au core–shell nanoparticles was also followed by UV-vis spectroscopy, X-ray diffraction and transmission electron microscopy measurements.

## Introduction

Nanomaterials have wide-ranging implications in a variety of areas, including chemistry, physics, electronics, optics, materials science and the biomedical sciences. Therefore, the development of synthetic protocols for nanomaterials over a range of chemical compositions constitute a steadily evolving branch of nanotechnology. The interest in core–shell nanoparticles is not just due to the enhancement of colloidal stability, but has also been driven by the interest in creating nanomaterials with unique and complex properties relative to the individual constituents. Such coatings in the core–shell morphology allow modification and tailoring of the particle properties (*e.g.*, optical, magnetic, catalytic) depending on the coating composition.[1] In principle, one can achieve precise control over the properties of these core–shell colloids by fine-tuning their chemical composition, structure, and dimensions of the cores and/or shells. Magnetic nanoparticles have applications in information storage,[2] color imaging,[3] magnetic refrigeration,[4] bio-processing,[5] medical diagnosis[6] and controlled drug delivery.[7] The latter applications require magnetic nanoparticles to be well-dispersed in liquid media, chemically stable and uniform in size. Due to the magnetic dipolar attraction, unmodified ferromagnetic nanoparticles tend to aggregate into clusters and inhibit the advantage of the specific properties of single nanoparticles. Such aggregation of ferromagnetic nanoparticles can be avoided by such methods as creating an electrostatic double layer,[8] using a surfactant steric stablizer,[9] or by shifting the isoelectric point with citric acid and silica coating.[10,11] The main difficulty for the use of pure metal magnetic nanoparticles such as Co, Ni, and Fe arises from their instability toward oxidation in air, which becomes worse as their size gets smaller. In addition, these metallic magnetic nanoparticles are bio-hazardous as well. Therefore, it is important to develop methods to both improve their chemical stability and, for various biomedical applications of the particles, the coating of their surface with a thin protecting shell. One approach for chemical stabilization is the deposition of insulating shells on the nanoparticles surface that prevent the reaction of oxygen with the surface atoms. Usually, an inert silica coating on the surface of magnetic nanoparticles reduces their aggregation in a liquid and improves the chemical stability.[12] At the same time, the silanol surfaces can be modified with various coupling agents to covalently attach specific bio-ligands to the surfaces of the magnetic nanoparticles.[13] As an alternative to silica, noble metals can also be deposited on the magnetic particles.[14] There are several advantages to be gained from using a gold coating as the shell on the magnetic-core nanoparticles, such as easy surface modification that allows the preparation of non-aqueous colloids and the easy control of interparticle interactions, both in solution and within structures through shell thickness. Furthermore, if the shell can provide additional functionality, such as sensitivity to optical probes and other biomolecules, it would be highly desirable for a number of applications. Generally, core–shell nanoparticles can be synthesized by successive reduction of one metal ion over the core of another metal ion.[15] However, this process may also lead to the formation of fresh nuclei of the second metal ion in addition to a shell around the first metal core, which is undesirable from an application point of view. To overcome this drawback, a strategy has been developed for the immobilization of a reducing agent on the surface of the core metal which, when exposed to the second metal ions, would reduce them and form a thin metallic shell on the surface of the core. Such displacement reactions are a good choice for synthesizing the phase-pure magnetic core–shell nanoparticles, where the surface of the magnetic nanoparticle is sacrificed as

*Department of Materials Science & Engineering, University of Washington, Seattle, Washington, 98195, USA.*
*E-mail: kannanmk@u.washington.edu*

 

the reducing agent for the noble metal deposition on the surface of the core nanoparticles.[16] It is well known that extrinsic magnetic properties such as coercivity depend on the size of the magnetic nanoparticles.[17] Since, in this displacement reaction, the nanoparticle surface functions as the reducing agent and is progressively sacrificed, its core size will decrease with time. Hence, here we demonstrate, in addition to routine optical measurements and structural characterization, a novel but sensitive magnetic method to monitor the formation of core–shell nanoparticles by measuring the hysteresis (determining coercivity and remanence) as a function of reaction time during the course of the formation of Co-core Au-shell nanoparticles by displacement reaction.

## Experimental

### Chemicals

Chloroauric acid ($HAuCl_4$), tetraoctylammonium bromide (TOAB) [$(C_8H_{17})_4N^+$ $Br^-$], decacarbonyl dicobalt ($Co_2(CO)_{10}$), 1,2-dichlorobenzene (DCB), trioctylphosphine oxide (TOPO).

### Synthesis of cobalt nanoparticles

The synthesis of cobalt nanoparticles was performed under an argon atmosphere by rapid decomposition of cobalt carbonyl in the presence of a capping agent. In a typical experiment, 1.58 mmol (0.54 g) of cobalt carbonyl dissolved in 3 mL of DCB was injected into 14 mL DCB containing 0.26 mmol (0.1 g) of TOPO at 182 °C and refluxed for 1 h. This produces ferromagnetic cobalt nanoparticles, 18–20 nm in diameter, with a narrow size distribution and individually stabilized by the surfactant coating.[18]

### Preparation of hydrophobized gold ions ($[(C_8H_{17})_4N]^+$ $[AuCl_4]^-$)

20 mL of an aqueous solution of $10^{-2}$ $HAuCl_4$ was placed in a beaker along with 20 mL of $10^{-2}$ M TOAB (tetraoctylammonium bromide) in DCB and the biphasic mixture was stirred for 5 h. At the end of this reaction, the appearance of an orange color in the organic phase could clearly be seen, indicating phase transfer of $AuCl_4^-$ ions into DCB, and the organic phase was separated from the aqueous phase for further reactions.

### Synthesis of Co@Au core–shell nanoparticles

4 mL of a solution of phase-transferred hydrophobized gold ions in DCB ($[(C_8H_{17})_4N]^+$ $[AuCl_4]^-$) was heated at 90 °C in a round-bottomed flask under argon atmosphere, and at that temperature, 2 mL of as-synthesized cobalt nanoparticles in DCB were injected into the gold ion solution and stirred for 2 h. Reaction mixtures were collected for magnetic measurements at different times such as $t = 0$ (immediately after addition of Co nanoparticles into the $[(C_8H_{17})_4N]^+$ $[AuCl_4]^-$ solution), 30 min, 60 min, 90 min and 120 min. After collecting the reaction mixtures at the different collection times, the reaction was quenched by adding dry absolute ethanol and the samples were collected by centrifugation.

**UV-vis spectroscopic studies.** UV-vis spectra of the cobalt and Co@Au core–shell nanoparticle solutions in DCB were measured on a Carry 550 UV-vis spectrophotometer, operated at a resolution of 2 nm.

**X-Ray diffraction measurements.** X-Ray diffraction (XRD) analysis of drop-coated films on glass substrates from the Co and Co@Au core–shell nanoparticles were carried out on a Rigaku Rotaflex instrument, operating at 50 kV and a current of 150 mA with Cu-K$\alpha$ radiation.

**Magnetic measurements.** Magnetic hysteresis of Co and different stages of Co@Au core–shell formation were measured using a Lake Shore vibrating sample magnetometer at 300 K.

**Transmission electron microscopy (TEM) measurements.** Samples for TEM studies were prepared by placing a drop of the Co and Co@Au core–shell nanoparticle solutions on carbon-coated TEM grids. The films on the TEM grids were then allowed to dry. TEM measurements were carried out on a Philips EM 420 instrument at an accelerating voltage of 120 kV.

## Results and discussion

Co@Au core–shell nanoparticles were synthesized by the displacement reaction between surface atoms of Co nanoparticles and $Au^{3+}$ of hydrophobized gold ions ($[C_8H_{17})_4N]^+$ $[AuCl_4]^-$). The process of the gold shell formation by reduction of the $Au^{3+}$ of $AuCl_4^-$ ions on the surface of cobalt core nanoparticles was followed by UV-vis spectroscopy. Fig. 1 shows the UV-vis absorption spectra recorded from pure cobalt nanoparticles (curve 1) and after 2 h of addition of hydrophobized $AuCl_4^-$ ions (curve 2). Prior to addition of hydrophobized $AuCl_4^-$ ions into the Co nanoparticle solution, it is observed that there is no absorption in the visible region of the electromagnetic spectrum[19] (curve 1) whereas, after addition of hydrophobized $AuCl_4^-$ ions, a

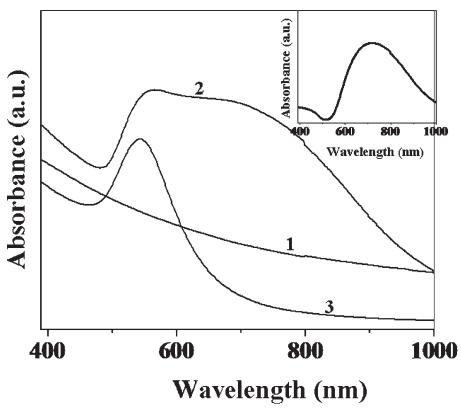


**Fig. 1** UV-vis spectra recorded from: curve 1, cobalt nanoparticle solution; curve 2, as-synthesized Co@Au nanoparticle solution; curve 3, aqueous solution of pure $CoCl_2$. The inset shows the UV-vis spectrum after subtracting curve 3 from curve 2 in the main figure (see text for details).

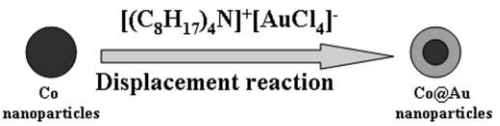


**Scheme 1** Redox reaction: $n$Co + $[(C_8H_{17})_4N]^+$ $[AuCl_4]^-$ = $Co_{(n-1)}$@Au + $CoCl_2$ + $[(C_8H_{17})_4N]^+$ $Cl^-$

broad absorption band from the sample centered at *ca.* 550 and 715 nm can be clearly seen (curve 2). To evaluate the origin of the two absorption peaks in curve 2, we separately measured the absorption spectrum of an aqueous solution of pure $CoCl_2$ (since the by-product, mainly $CoCl_2$, is formed during the displacement reaction, see Scheme 1) and curve 3 shows the absorption band centered at *ca.* 550 nm due to absorbance of $CoCl_2$ solution. Comparing curves 2 and 3, it is clear that the absorption band at 550 nm in curve 2 comes from the by-product of the reaction, and the absorption band centered at 715 nm can be attributed to surface plasmon excitations in the gold shell formed around the cobalt core. For clarity, by subtracting the contribution of pure $CoCl_2$ (the by-product; curve 3) from the total signal (Co@Au *and* by-product), we show (inset of Fig. 1) only the absorption spectrum of Co@Au core–shell nanoparticles. The large red shift observed in the position of the plasmon resonance, attributed to the formation of a gold shell instead of free gold nanoparticles in the displacement reaction, is consistent with values for gold-coated nanoparticles reported in the literature.[20]

Fig. 2 shows the XRD pattern of as-synthesized Co nanoparticles (curve 1) and Co-core Au-shell nanoparticles (curve 2). In curve 1, the peak positions at $2\theta$ = 44.8, 47.1 and 49.5° can be indexed as $\varepsilon$-cobalt.[21] No distinct peak corresponding to CoO is detected, indicating that single-phase $\varepsilon$-cobalt is obtained. All peaks in curve 2 can be indexed as FCC gold.[22] The cobalt peaks are not clearly resolved, probably due to the enhanced scattering from the gold as a result of the formation of Au-coated Co nanoparticles. The fact that the diffraction peaks from the core in the core–shell nanoparticles were absent is consistent with reports in the literature,[22] and provides evidence of complete coverage of the cobalt core by gold in the Co@Au core–shell nanoparticles.

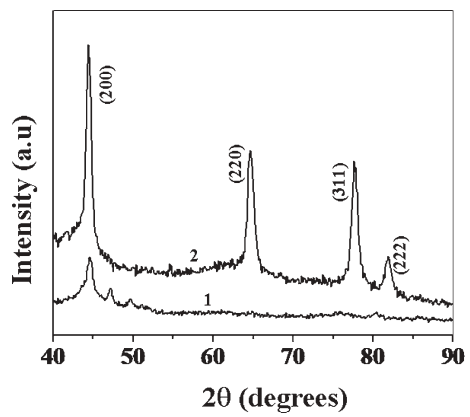


**Fig. 2** XRD patterns recorded from drop-coated films on glass substrates of cobalt nanoparticles (curve 1), Co@Au core–shell nanoparticles (curve 2) in the $2\theta$ range 400–900.

It is very difficult to unequivocally confirm the formation of a shell on the surface of core nanoparticles in the displacement reaction. Typically, high resolution TEM imaging is used but this is constrained by very limited sampling. However, extrinsic magnetic properties, such as coercivity, $H_c$, critically depend on the size of the magnetic nanoparticles. For example, up to a diameter of ~10 nm, cobalt nanoparticles exhibit superparamagnetic ($H_c$ = 0) behavior, and as their size increases further, they are not only ferromagnetic (open hysteresis loops) but their coercivity increases rapidly to a maximum value for a size of ~18–20 nm. In other words, measuring the change in the magnetic coercivity of the cobalt nanoparticles would be a sensitive monitor of the formation of Au-shell on the surface of the magnetic-core in the displacement reaction, especially if the shell is formed due to the sacrifice of the surface of the core to promote the reduction of metal ions. Fig. 3(A–E) shows the kinetics of the size dependent hysteresis ($M$ *vs.* $H$) loops at 300 K during the formation of Co-core Au-shell nanoparticles in the displacement reaction at times of 0, 30, 60, 90 and 120 min, respectively. As the size of the magnetic core decreases during the course of the displacement reaction, the coercivity ($H_c$) or the width of the hysteresis loop of the Co-core nanoparticles decreases systematically (values of 322, 300, 247, 91 and 82 Oe are obtained for 0, 30, 60, 90 and 120 min, respectively). Care was taken to saturate the particle (insets, Fig. 3(A–E)) by applying large enough fields for all the measurements. Fig. 3F shows the systematic decrease of coercivity ($H_c$) as a function of reaction time ($T$). This decrease in $H_c$ can be correlated directly with decreasing size of the Co core during the formation of the Au shell by the reduction of gold ions on its surface in the displacement reaction. There is a chance that the decrease in coercivity ($H_c$) of the Co-core nanoparticles may be due to the oxidation of the surface of cobalt atoms. We have ruled out this possibility, since the gold ions would not be reduced on a CoO surface and our other measurements, *i.e.* UV-vis spectroscopy and XRD, support the formation of a gold shell. From our experimental section, it is clear that no external reducing agents were used for the reduction of gold ions; it was accomplished by sacrificing the surface of the core cobalt nanoparticles and, thus, there was no possibility of the formation of any fresh gold nuclei.

TEM was used to obtain images of starting Co-core nanoparticles (Fig. 4A) and Co@Au core–shell (Fig. 4B) nanoparticles. From Fig. 4A, it is seen that cobalt nanoparticles are uniform, with sizes ranging from 18–20 nm. Comparing Fig. 4A and Fig. 4B, it is seen that for pure cobalt nanoparticles (Fig. 4A) the contrast is uniform throughout the particle, whereas for Co-core Au-shell nanoparticles (Fig. 4B) there is a distinct variation in contrast between the dark cobalt core and the lighter gold shell. In the TEM images of the core–shell morphology, mass contrast appears to dominate over diffraction contrast, rendering the shell lighter even though Au has a higher atomic number than Co. From the TEM image of Co@Au nanoparticles (Fig. 4B), it is observed that even though the average size of the Co-core has decreased compared to the starting cobalt nanoparticles (Fig. 4A), the average size of the Co@Au core–shell nanoparticles remains similar to that of the starting Co nanoparticles.

 

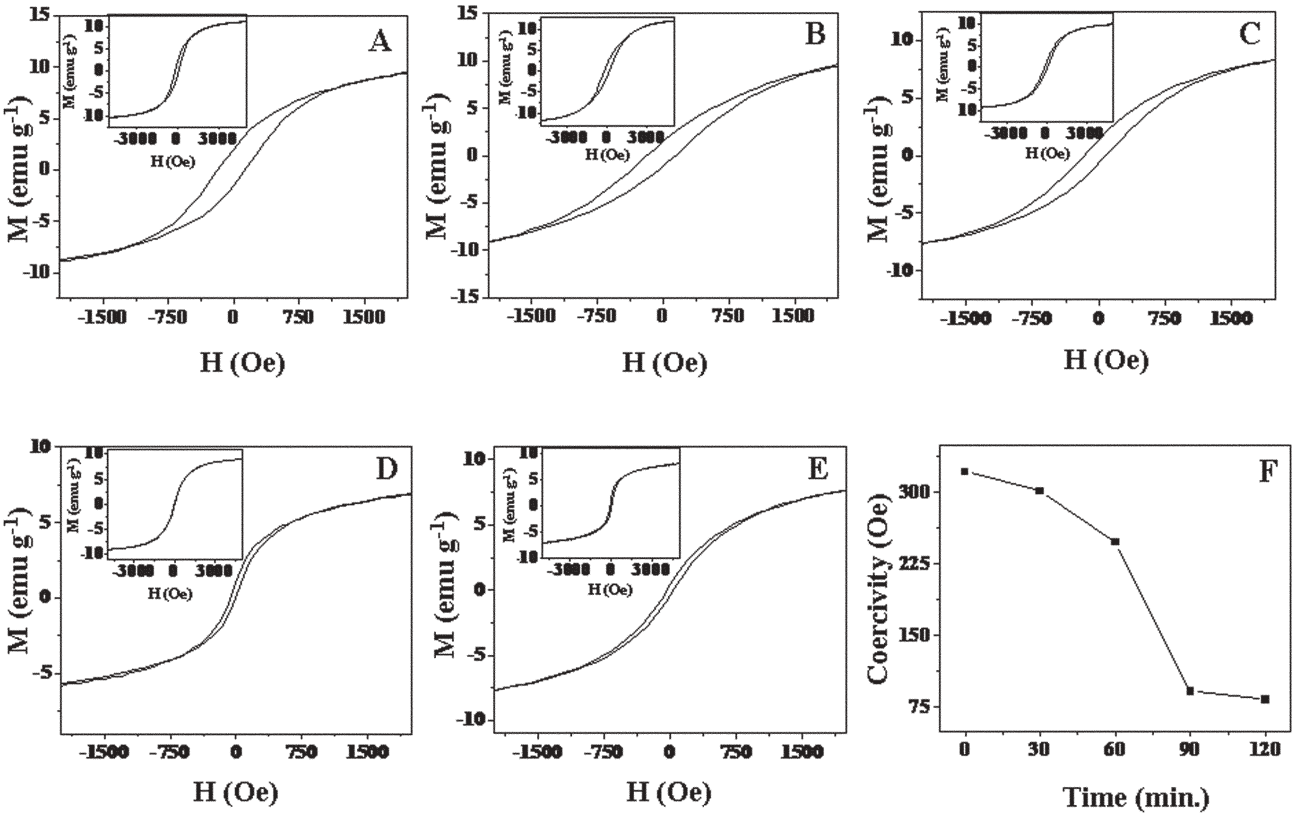


**Fig. 3** (A–E) show the magnetization *vs.* field (*M vs. H*) hysteresis loops at 300 K for Co@Au reaction mixtures in the displacement reaction at times of 0, 30, 60, 90 and 120 min, respectively. The insets of (A–E) show the hysteresis curves, at full scale, of the high field region at 300K. (F) shows the plot of coercivity ($H_c$) measured from the hysteresis loops of (A–E) *vs.* time (*T*).

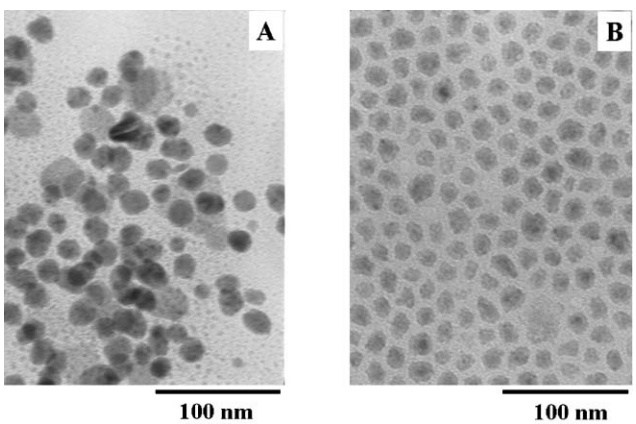


**Fig. 4** Representative TEM pictures of (A) Co nanoparticles and (B) Co@Au core–shell nanoparticles.

## Conclusion

In conclusion, the formation of Co-core Au-shell nanoparticles using the displacement method has been described. Our experimental results show the formation of a gold shell on the cobalt core nanoparticles by a redox transmetalation reaction without the need of additional reducing agent, where the surface of the cobalt acts as a reducing agent for the reduction of gold ions. As the gold shell grows on the cobalt core, a stoichiometric fraction of cobalt metal is replaced by gold through a displacement process, and this is supported by the standard potential values of $Co^{2+}/Co$ (−0.28 V) and $Au^{3+}/Au$ (1.83 V) systems. A significant advantage of this method is the ability to control the core-size by controlling the molar ratio of cobalt metal to gold ions. Measurement of the magnetic hysteresis of the core–shell nanoparticles provides a direct method of monitoring the decrease in core-size as the displacement reaction proceeds.

## Acknowledgements

This work is supported by NSF (DMR-0501421) and the Campbell Endowment at UW.

## References

1 (*a*) F. Caruso, *Adv. Mater.*, 2001, **13**, 11; (*b*) S. R. Hall, S. A. Davis and S. Mann, *Langmuir*, 2000, **16**, 1454.
2 (*a*) J. C. Lodder, *J. Magn. Magn. Mater.*, 2004, **272**, 1692; (*b*) R. J. Hicken, *Philos. Trans. R. Soc. London, Ser. A*, 2003, **361**, 2827.
3 R. F. Ziolo, *U.S. Pat.* 4,474,866, 1984.
4 (*a*) Y. Yang, J. Chen, J. He and E. Bruck, *Physica B (Amsterdam)*, 2005, **364**, 33; (*b*) V. Franco, J. S. Blázquez, C. F. Conde and A. Conde, *Appl. Phys. Lett.*, 2006, **88**, 042505.
5 N. M. Pope, R. C. Alsop, Y. A. Chang and A. K. Sonith, *J. Biomed. Mater. Res.*, 1994, **28**, 449.
6 L. Josephson, C. H. Tsung, A. Moore and R. Weissleder, *Bioconjugate Chem.*, 1999, **10**, 186.
7 S. P. Bhatnagar and R. E. Rosensweig, *J. Magn. Magn. Mater.*, 1995, **149**, 198.

8 M. H. Sousa, J. C. Rubim, P. G. Sobrinho and F. A. Tourinho, *J. Magn. Magn. Mater.*, 2001, **225**, 67.
9 C. Rocchiccioli-Deltcheff, R. Franck, V. Cabuil and R. Massart, *J. Chem. Res.*, 1987, 126.
10 A. Bee and R. Massart, *J. Magn. Magn. Mater.*, 1990, **122**, 1.
11 A. P. Philipse, M. P. van Bruggen and C. Pathmamanoharan, *Langmuir*, 1994, **10**, 92.
12 Y. Kobayashi, M. Horie, M. Konno, B. R-Gonzalez and L. M. Liz-Marzan, *J. Phys. Chem. B*, 2003, **107**, 7420.
13 (*a*) Q. Liu, J. A. Finch and R. Egerton, *Chem. Mater.*, 1998, **10**, 3936; (*b*) A. Ulman, *Chem. Rev.*, 1996, **96**, 1533.
14 (*a*) M. Mandal, S. Kundu, S. K. Ghosh, S. Panigrahi, T. K. Sau, S. M. Yusuf and T. Pal, *J. Colloid Interface Sci.*, 2005, **286**, 187; (*b*) Q. H. Lu, K. L. Yao, D. Xi, Z. L. Liu, X. P. Luo and Q. Ning, *J. Magn. Magn. Mater.*, 2006, **301**, 44.
15 T. Kinoshita, S. Seino, K. Okitsu, T. Nakayama, T. Nakagawa and T. A. Yamamoto, *J. Alloys Compd.*, 2003, **359**, 46.
16 (*a*) J.-I. Park and J. Cheon, *J. Am. Chem. Soc.*, 2001, **123**, 5743; (*b*) W.-r. Lee, M. G. Kim, J.-r. Choi, J.-I. Park, S. J. Ko, S. J. Oh and J. Cheon, *J. Am. Chem. Soc.*, 2005, **127**, 16090.
17 Y. K. Su, C. M. Shen, T. Z. Yang, H. T. Yang, H. J. Gao and H. L. Li, *Appl. Phys. A*, 2005, **81**, 569.
18 Y. Bao, A. B. Pakhomov and K. M. Krishnan, *J. Appl. Phys.*, 2005, **97**, 10J317.
19 (*a*) C. Petit and M. P. Pileni, *J. Magn. Magn. Mater.*, 1997, **166**, 82; (*b*) D. E. Cliffel, F. P. Zamborini, S. M. Gross and R. W. Murray, *Langmuir*, 2000, **16**, 9699.
20 (*a*) W. Shi, Y. Sahoo, M. T. Swihart and P. N. Prasad, *Langmuir*, 2005, **21**, 1610; (*b*) Y. Sun, B. T. Mayers and Y. Xia, *Nano Lett.*, 2002, **2**, 481; (*c*) J. B. Jackson and N. J. Halas, *J. Phys. Chem. B*, 2001, **105**, 2743.
21 C. B. Murray and S. Sun, *J. Appl. Phys.*, 1999, **85**, 4325.
22 L. Wang, J. Luo, Q. Fan, M. Suzuki, I. S. Suzuki, M. H. Engelhard, Y. Lin, N. Kim, J. Q. Wang and C.-J. Zhong, *J. Phys. Chem. B.*, 2005, **109**, 21593.



 